THERMOHYDRAULIC MODELING OF AN ELECTRO-HYDRAULIC SERVO ACTUATOR ON DAMPED MODE

Marina Brasil Pintarelli
ITA, Embraer
mabrapin@gmail.com
São José dos Campos, SP, Brazil

Emília Villani
ITA
evillani@ita.br
São José dos Campos, SP, Brazil

Ronaldo Horácio Cumplido Neto
Embraer
ronaldo.neto@embraer.com.br
São José dos Campos, SP, Brazil

ABSTRACT

Hydraulically powered flight control systems are widely used in aviation, especially for commercial aircraft, which require significant forces from system actuators to control the applicable surfaces as demanded. These systems are being studied and are evolving to become smaller, lighter, and more efficient. These improvements bring several advantages, such as payload increase and drag reduction. However, as these systems are optimized, and their dimensions are reduced, the thermal effects of fluid flow become more relevant. Especially when the working fluid passes through small orifices, excessive heat can eventually compromise the equipment's performance and damage its internal subcomponents. When we analyze the damped mode operation of actuation systems presented on some commercial aircraft, these restrictions become even more relevant – knowing that the damping orifice diameter can be significantly reduced to provide the desired performance for the operation. Therefore, the main goal of this study is to analyze and evaluate the thermal impact on an Electro-Hydraulic Servo Actuator (EHSA) while in damped mode operation, contributing to the industry and the literature in this kind of assessment. Through the research presented, it's possible to estimate the temperature of the system's components and, consequently, avoid malfunctions caused by overheating. Furthermore, developing a model allows the simulation of various environmental conditions, reducing rig costs or in-flight tests. The modeling approach was conducted on the MATLAB/Simulink platform. It was based on two main points that improved model comprehension during its development and minimized errors: the building blocks philosophy of segregating each component's influence and model, and the continuous validation of the model through a comparison with a physics-integrated software (AMESim).
[DOI: https://doi.org/10.3384/ecp196005]

Keywords: *flight control system, thermohydraulic modeling, damped operation, electro-hydraulic servo actuator (EHSA)*

INTRODUCTION

Hydraulically powered flight control systems are widely used in aviation, mainly for primary and secondary flight control surfaces. The primary surfaces are essential for aircraft control and must meet safety requirements, leading to complex architectures. One requirement is to have redundancies to guarantee a low failure probability [1]. Usually, the redundancy required in a flight control system can be met with two actuators for each primary surface with independent power sources [2]. Depending on the aircraft design, the operating flight control system mode is called active-active (both actuators apply force at the surface) or active-standby (one actuator activated and one on standby). The redundancy configuration is chosen during aircraft development due to weight, performance, and load requirements.

For both configurations (active-active and active-standby), if there is a failure in one actuator, the faulty actuator goes into the damped or bypass mode, and the remaining actuator needs to be engaged. However, during this operation, the interaction between actuators' dynamic damping and/or stiffness with the aeroelastic characteristics of the aircraft wing is impacted. Thereby, the vibratory behavior of the system is affected. If vibrations at specific frequencies occur, they can increase in case there is no energy dissipation from the system, resulting in a catastrophic aircraft failure. Thus, during the design of flight control system components, mainly primary actuators, a damped valve, which embeds a calibrated orifice, can provide damping forces to change the vibratory behavior of the system precluding a flutter.

 Proceedings of the 6th Workshop on Innovative Engineering for Fluid Power – WIEFP 2022, 22-23 November 2022. ABIMAQ, São Paulo, SP, Brazil.

The damper effect is due to the passage of hydraulic fluid between the actuator chambers through a mode select valve. From the system design point of view, active-active has two operating modes: normal operation (when both actuators are suitable for operation) and operation with failure (when one of the actuators has a fault) [3]. Figure 1 shows the main components of the flight control hydraulic system. In this case, its mode select valve determines whether the mode is active, bypassed, or damped. Figure 1 represents the Solenoid Valve (SOV) not energized, consequently the Mode Select Valve (MSV) is not actuated and remains in the damped position for the analyzed system.

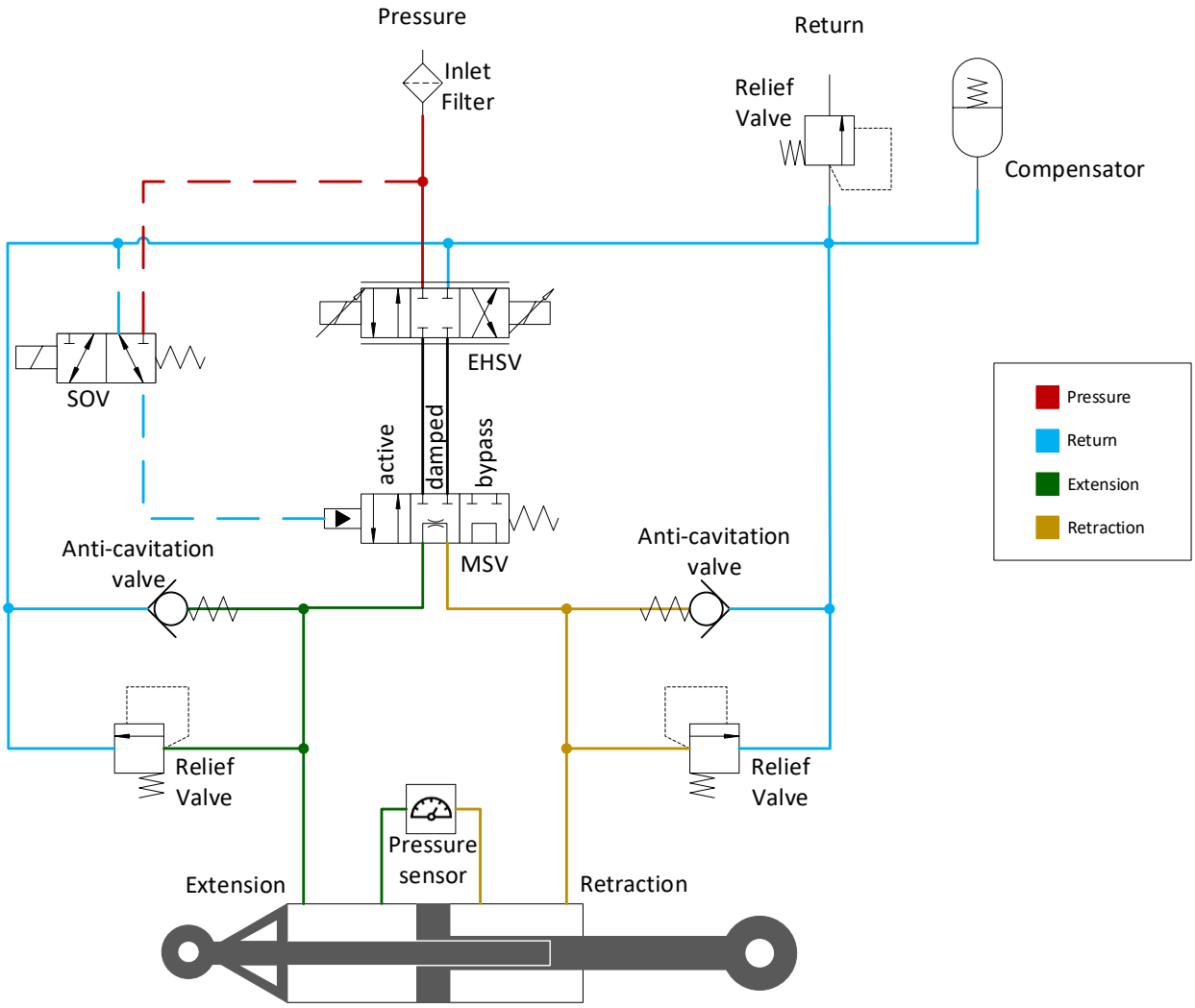

Figure 1 – Actuation architecture comprising active, bypass, and damped modes of an electro-hydraulic servo actuator.

Fluid passing through small orifices can impact the temperatures of the hydraulic system and consequently compromise the equipment's performance and damage its internal subcomponents. Previous studies discussed the influence of temperature variation on the system time and frequency response and aeroelastic requirements [2][4] or the temperature behavior of the hydraulic system during normal operation [5][6][7][8][9].

This study focuses on modeling the thermal behavior of the main components of a flight control system in the damped operation of a certified civil aircraft. The analysis was selected since the damped orifice can have restricted dimensions and may cause fluid heating inside the system. Also, the behavior can be amplified as the fluid is restricted to the manifold lines and cycled in this operation. The configuration investigated has a complete fly-by-wire control system, and its actuators are electro-hydraulic (actuation is hydraulically powered, and control is electro-electronically). The actuation surface is a primary surface type and features redundancy with two actuators in operation to carry out the flight demands. The hydraulic fluid is a fire-resistant phosphate ester hydraulic fluid type IV detailed at the standard SAE AS1241 [10].

THERMAL HYDRAULIC MODEL

The modeling was developed considering the main components of the hydraulic system in damped mode operation, and some simplifications were performed. Figure 2 represents the components modeled to evaluate the thermal behavior: the damping orifice of the mode select valve, two anti-cavitation valves, two relief valves, one balanced actuator with two chambers, and the return line. The compensator and the relief valve linked to the return line were not modeled; thus, the temperature of the return was considered the average value of the return temperature and the chambers mean temperature.

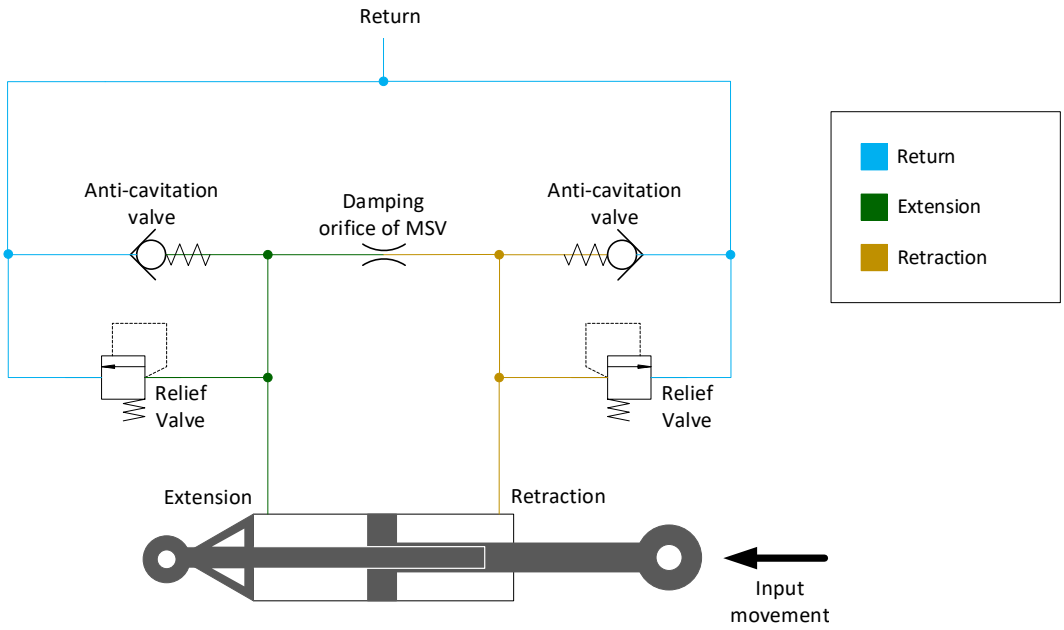

Figure 2 – Simplified damped hydraulic system.

Also, the input of the model is the position of the actuator stroke, as a position sensor often measures it. The model converted this input into stroke speed and consequently into the volumetric rate of the actuator chambers. The volume change generated a pressure difference between the chambers and a mass flow rate.

Two fundamental elements describe the physical behavior of thermohydraulic systems: capacitive and resistive blocks [6]. The following subsections detail the mathematical modeling of both.

Resistive Elements

Two equations govern the thermohydraulic behavior of resistive elements (e.g., restrictions). The first calculates the mass flow in the region – Equation (1) –, and the second the temperature increase – Equation (3). Because of viscous friction, a coefficient is introduced for the mass flow to address the power loss effects [11]. The discharge coefficient (c_q) is a dimensionless number, function of the characteristics of the flow, and geometric aspects of the orifice. The mass flow rate equation is indicated by Equation (1) [12].

$$\dot{m} = \rho \cdot c_q \cdot A \cdot \sqrt{\frac{2}{\rho}(p_1 - p_2)} \tag{1}$$

The enthalpy equation for thermohydraulic fluids can be written as Equation (2), a function of the temperature derivative (dT/dt) and the pressure derivative (dp/dt) [6].

$$\frac{dh}{dt} = c_p \frac{dT}{dt} + \frac{(1 - \alpha T)}{\rho} \frac{dp}{dt} \tag{2}$$

Considering that the heat generated by the restriction is transferred to the fluid, the transformation can be classified as isenthalpic. Thereby, it is possible to estimate the temperature variation in the fluid using Equation (2) and considering that the derivative of the enthalpy (dh/dt) is zero as shown in Equation (3).

$$T_{out} = T_{in} + \frac{(1 - \alpha T_{in}) \cdot |\Delta p|}{\rho \cdot c_p} \tag{3}$$

Capacitive Element

The fundamental capacitive element is considered a control volume with variable volume (e.g., each actuator chamber). Two equations govern the thermohydraulic behavior of capacitive elements: The first relates the pressure variation to the temperature and density variation using two experimental parameters (the bulk modulus and the expansion coefficient) – Equation (10) –, and the second estimates the temperature rise – Equation (15).

The mass variation inside a control volume (dm/dt) is the difference between the mass flow rate entering and the mass flow rate leaving the volume. The mass of a control volume (m) is given by its density (ρ) multiplied by its volume (V). Equation (4) evaluates the derivative of the equation, a relation between the derivatives of mass (dm/dt), volume (dV/dt), and density ($d\rho/dt$) [12].

$$\frac{dm}{dt} = \rho \frac{dV}{dt} + V \frac{d\rho}{dt} \tag{4}$$

In addition to density, properties such as kinematic viscosity, specific heat, volumetric expansion coefficient, and bulk modulus are a function of the pressure and temperature of the fluid. The density (ρ) is a function of pressure (p) and temperature (T). With partial derivatives, the relation of Equation (5) is obtained [12].

$$d\rho = \left(\frac{\partial \rho}{\partial p}\right)_T dp + \left(\frac{\partial \rho}{\partial T}\right)_p dT \tag{5}$$

To address the density variation, two empirical quantities of fluids - the bulk modulus (β) and the thermal expansion coefficient (α) - relate pressure, temperature, and density variations. Equation (5) was manipulated to highlight these parameters.

$$dp = \frac{\rho}{\left(\frac{\partial \rho}{\partial p}\right)_T} \cdot \left[\frac{d\rho}{\rho} - \frac{1}{\rho}\left(\frac{\partial \rho}{\partial T}\right)_p \cdot \mathrm{dT}\right] \tag{6}$$

The thermal expansion coefficient (α) is a volumetric expansion coefficient that describes a fluid's contraction or expansion with a specific temperature change. It is calculated as a function of density (ρ) and temperature (T) [11].

$$\alpha(\mathrm{p}, \mathrm{T}) = -\frac{1}{\rho} \cdot \frac{\partial \rho}{\partial \mathrm{T}} \tag{7}$$

One of the most relevant properties of flight control system is the bulk modulus. The bulk modulus is a term used to denote fluid resistance to uniform compression [13]. The selection of the proper bulk modulus is based on the function performed. AIR 1362 (2008) suggests that dynamic systems with small pressure excursions, *e.g.*, oscillating servo actuators, shall be modeled using the adiabatic tangent module (β_t) showed in Equation (8).

$$\beta_t = -\mathrm{V} \cdot \frac{\partial \mathrm{p}}{\partial \mathrm{V}} = \rho \frac{\partial \mathrm{p}}{\partial \rho} \tag{8}$$

The tangent bulk modulus (β_t) is calculated using the derivative of pressure (p) and volume (V) or as a function of the density (ρ) and the pressure (p). Returning to Equation (6) and applying Equations (7) and (8), Equation (9) is obtained:

$$\frac{dp}{dt} = \beta_t \left(\frac{1}{\rho}\frac{d\rho}{dt} + \alpha \frac{dT}{dt}\right) \tag{9}$$

This equation relates the pressure variation (dp/dt) with two empirical parameters – the bulk modulus (β) and the volumetric expansion coefficient (α) – and with the density ($d\rho/dt$) and temperature variation (dT/dt).

Combining expressions (4) and (9), Equation (10) is obtained. The relation for the derivative of the pressure is a function of the bulk modulus (β), the mass flow rate balance ($\Sigma(\dot{m})$), the density (ρ), the volume derivative (dV/dt), the volume (V), the thermal expansion coefficient (α) and the temperature derivative (dT/dt).

$$\frac{dp}{dt} = \beta\left(\frac{\Sigma(\dot{m}) - \rho\frac{dV}{dt}}{\rho V} + \alpha\frac{dT}{dt}\right) \tag{10}$$

For temperature evaluation, the first law of thermodynamics is used. The system's energy variation (ΔE) is a function of the heat transferred to the system (Q) and the work applied or done by the system (W). When applied to control volumes, the equation of the first law can be written as Equation (11) [14]:

$$\frac{dE}{dt} = \dot{Q} - p\frac{dV}{dt} + \sum\dot{m}h \tag{11}$$

Also, the mass enthalpy (mh) is the sum of the internal energy (U) and the product of the pressure and volume (PV) of a thermodynamic system [15]:

$$mh = U + pV \tag{12}$$

The energy (E) inside the control volume is the sum of the internal energy (U), the kinetic energy, and the potential energy [6]. Thus, if the kinetic and potential energies are neglected, based on Equations (12), the time rate of change of the system's energy can be expressed as Equation (13).

$$\frac{dE}{dt} = \frac{dU}{dt} = \frac{d(mh - pV)}{dt} \tag{13}$$

Combining Equations (11) and (13), Equation (14) is obtained.

$$\frac{dh}{dt} = \frac{1}{\rho V}\left(\dot{Q} + \sum\dot{m}h - h\sum\dot{m}\right) + \frac{1}{\rho}\frac{dp}{dt} \tag{14}$$

Finally, combining Equations (2) and (14), the following relation is obtained:

$$\frac{dT}{dt} = \frac{\dot{Q} + \Sigma(\dot{m}\mathrm{h_i}) - h\cdot\Sigma(\dot{m})}{\rho\cdot c_p\cdot V} + \frac{\alpha\cdot T}{\rho\cdot c_p}\frac{dp}{dt} \tag{15}$$

Thermal exchanges

In addition to the thermohydraulic components, the manifold's heat exchanges, and thermal capacitances need to be addressed mathematically. For the modeling developed, the temperature on the surface of the chambers is calculated. The manifold is being evaluated with a simplified approach. The thermal capacitance between the fluid inside the chambers and the manifold surface is modeled as a single mass. Also, the resistive coefficients are modeled with an equivalent thermal coefficient.

With complex systems, it is possible to simplify the model and work with an overall heat transfer coefficient (U_t) [16]. This approach is used when intermediate temperatures are not an objective of the study. The transferred heat ($\dot{Q}$) is also dependent on the heat exchange area (A) and the temperature difference (ΔT).

In addition, an analogy exists between heat transfer and electrical systems. Electrical resistance is associated with the conduction of electricity; likewise, thermal resistance may be related to heat conduction. Therefore, the thermal resistance is defined as the ratio of a driving potential, the temperature difference (ΔT), to the corresponding transfer rate ($\dot{Q}$). The following equation summarizes the total thermal resistance (R_{tot}) as the sum of the resistances ($\sum R$) that are part of the heat transfer system. Also, the overall heat transfer coefficient (U_t) is related to the total thermal resistance and the heat exchange area (A).

$$R_{tot} = \sum R = \frac{\Delta T}{\dot{Q}} = \frac{1}{U_t A} \tag{16}$$

The equivalent capacitance (C_t) of a volume can be expressed as the material's specific heat multiplied by its mass.

$$\frac{dT}{dt} = \frac{\sum \dot{Q}}{mc_p} = \frac{\sum \dot{Q}}{C_t} \tag{17}$$

Modeling Platforms

Software such as MATLAB/Simulink or AMESim is often used to perform the simulations of dynamic models. MATLAB and Simulink combine textual and graphical programming to design in their simulation environment. AMESim is widely used for one-dimensional multi-domain system simulation by assembling and linking pre-defined components of a set of libraries. This research was mainly conducted in MATLAB/Simulink. However, AMESim was used to assess the results. This was possible since the AMESim libraries were developed and validated in cooperation with industrial partners, and the libraries are constantly being verified by the software users. In addition, the mathematical formulation of the blocks is available to users assess if the boundary conditions and hypotheses made during its development complies with the system to be modeled [17]. The comparison between software was very important in the development of the model because it was possible to identify modeling errors at the beginning of the development.

This modeling aims to be versatile for future developments; therefore, it was constructed by building each component separately. The Simulink model was developed based on two main blocks: the resistive (with equations (1) and (3)) and the capacitive (with equations (10) and (15). The blocks were linked by additional blocks representing the relations between the components of the system. Figure 3 shows the schematic of the Simulink model.

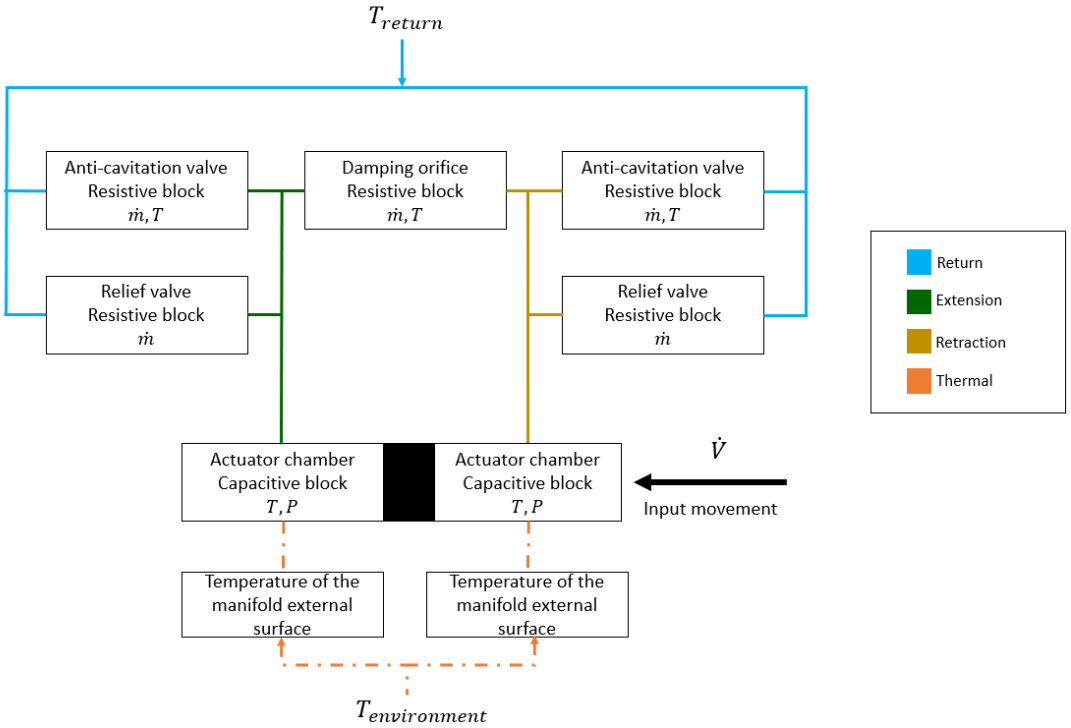

Figure 3 – Modeling schematic of Simulink with the blocks developed, classification (resistive or capacitive), and properties calculated.

The AMESim model was created using the thermal hydraulic library (damping orifice, anti-cavitation valves, and relief valves), the thermal hydraulic component design (actuator), and the thermal library (thermal capacitances and resistances). The complete model is represented in Figure 4.

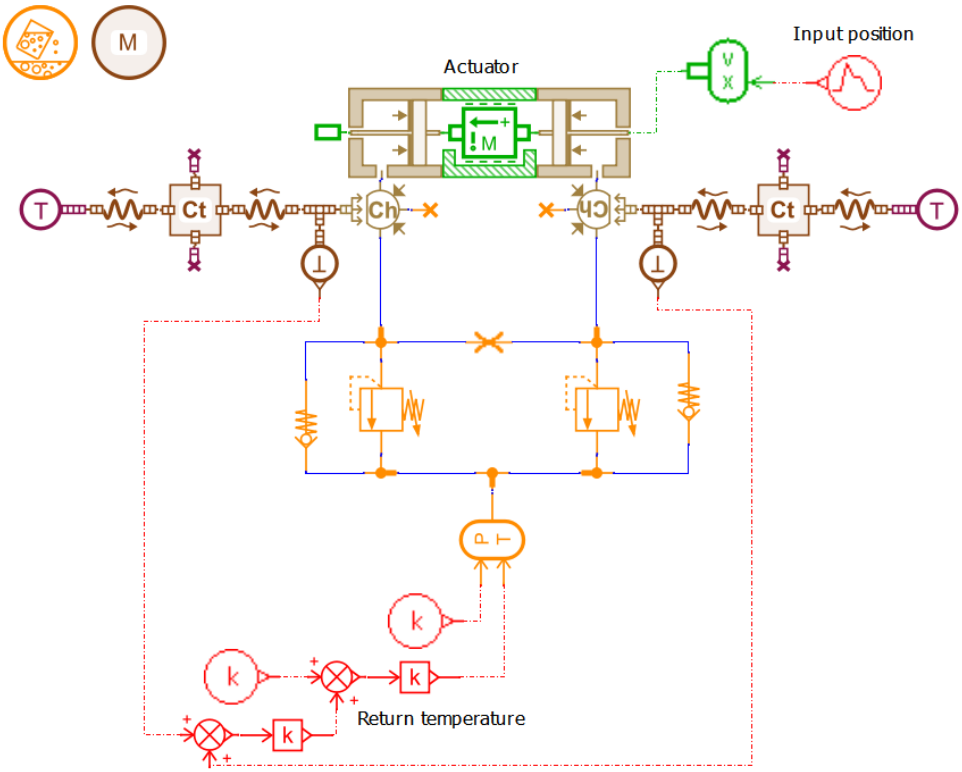

Figure 4 – AMESim complete model.

The main difference between both models is the fire-resistant phosphate ester hydraulic fluid type IV modeling. AMESim uses an embedded formulation based on higher-order polynomial functions. And MATLAB/Simulink formulation was developed based on the graphs of standard SAE AS1241 [10]. The equations presented in the previous subsections are valid for both MATLAB/Simulink and AMESim models [17].

RESULTS

Both models received the same input: five cycles initiating in the central position, reaching the retraction end, the extension end, and returning to the central position. The mean temperature of the chambers and the mean temperature of the external surface of the manifold were evaluated to compare the results.

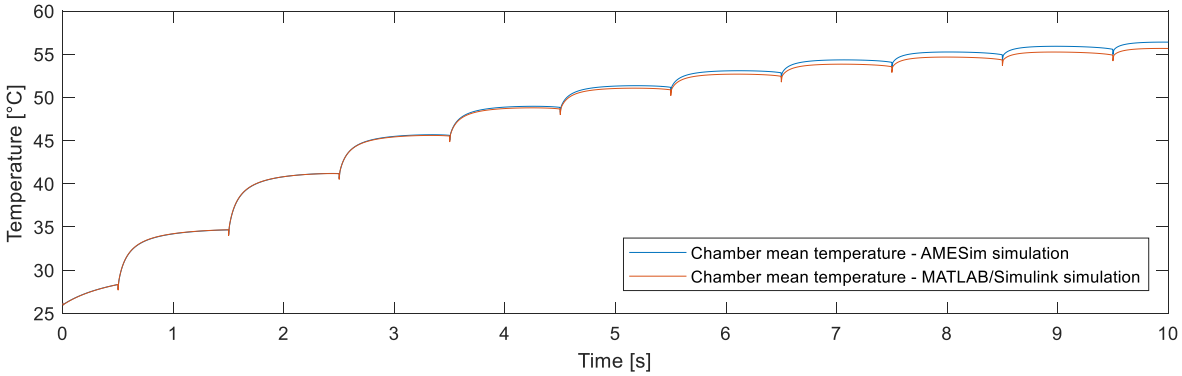

Figure 5 – Comparison of chambers mean temperature.

As shown in Figure 5, the behavior of both models was similar. The final value of the chambers average temperature simulated by MATLAB/Simulink had a percent variance of 1.3% from the AMESim result. And the surface temperature of the manifold obtained a difference of less than 1%, represented in Figure 6.

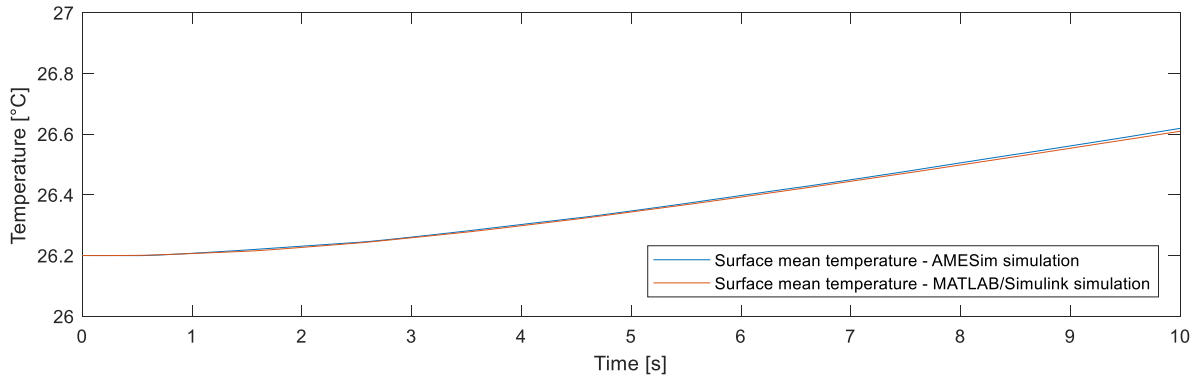

Figure 6 – Comparison of manifold surface temperature.

Software selection needs to be based on the research objective. The MATLAB/Simulink platform guarantees that all variables and implemented equations are known. However, the implementation of the equation is quite costly and subject to errors. AMESim has a more user-friendly interface; however, it has coupled physics. If the model designer does not study the details of modeling each component, some equations can be unintentionally added. Furthermore, for systems with many components, AMESim brings more advantages due to the model's speed of processing and development effort. However, the choice of a modeling platform is also a result of factors such as the number of licenses available in the organization.

Regarding the results, for the simulation performed, Figure 5 suggests that the chamber mean temperature reaches a plateau of around 55°C. Thus, superheating does not occur for the simulated case. The simulation was repeated with different thermal coefficients and higher operating pressure. Also, the cycles were extended to 200 seconds. The results are compiled in Figure 7.

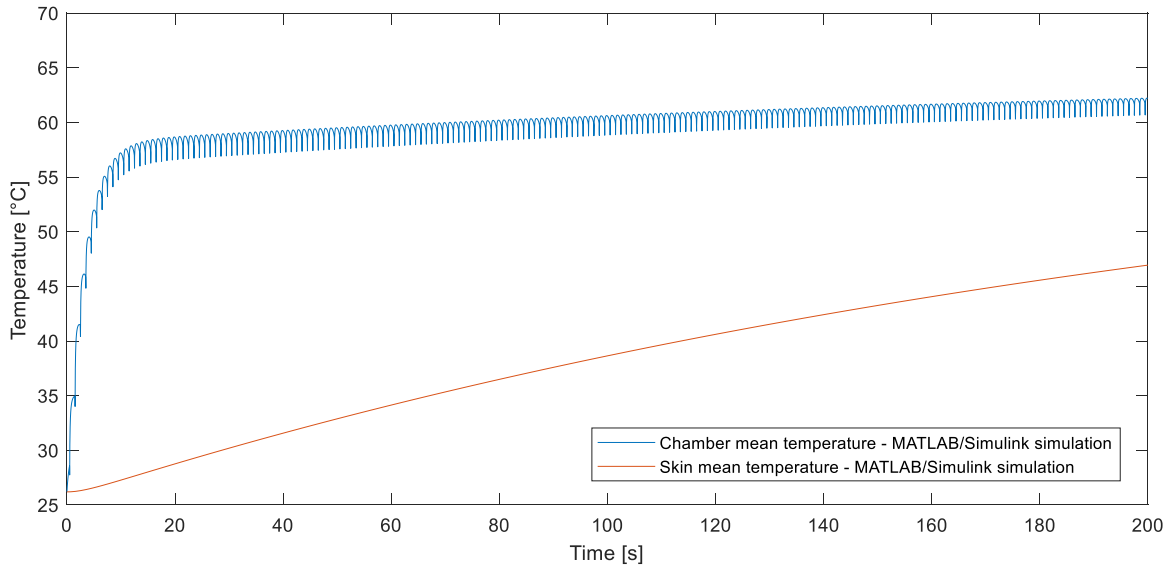

Figure 7 – Temperatures of second system condition simulated with MATLAB/Simulink.

Figure 7 shows that the chamber temperature reaches a higher plateau around 60°C and the manifold skin temperature is above 40°C due to the greater thermal coefficient. Moreover, the whole system elevates its temperature faster than the first case.

Analyzing an aircraft's flight envelope, performing a hundred cycles reaching the retraction end and the extension end of a primary flight control surface is not probable. However, a maintenance procedure or equipment test could require high cycling of the electro-hydraulic servo actuator. This simulation is an example of the capabilities of the model as it can evaluate the system temperature after design changes and for different operating conditions. In this way, it is possible to understand the impacts of the components dimensioning, geometry, and material changes on the system temperature. Also, the model can be applied to identify operation limitations such as the completion of a maintenance procedure that requires cycling with the electro-hydraulic servo actuator on damped mode.

CONCLUSION

Both models achieved satisfactory results, and it was possible to simulate the temperature of the manifold. A more detailed heat transfer assessment could more accurately evaluate the temperature of each component. In addition, it would be interesting to compare the results achieved with data from tests, perform a sensitivity analysis regarding the temperature impacts of each design change or perform a parametric identification to fit the models. However, the objectives of this research were achieved, and the models can be used to evaluate the flight control system operation in damped mode, focusing on predicting overheating.

NOMENCLATURE

A	Area
β	Bulk modulus
α	Coefficient of thermal expansion
ρ	Density
c_q	Discharge coefficient
EHSV	Electro-Hydraulic Servo Valve
E	Energy
h	Enthalpy
C_t	Equivalent capacitance
$\dot{Q}$	Heat transfer rate
U	Internal energy
m	Mass
$\dot{m}$	Mass flow
MSV	Mode Select Valve
U_t	Overall transfer coefficient
p	Pressure
SOV	Solenoid Valve
c_p	Specific heat at constant pressure
T	Temperature
R	Thermal resistance
t	Time
R_{tot}	Total thermal resistance
V	Volume

ACKNOWLEDGMENTS

The authors thank Fundação Casimiro Montenegro Filho (FCMF) and Embraer for funding the research.

REFERENCES

[1] UNITED STATES. Federal Aviation Administration 14 CFR- Part 25 Subpart D: design and construction: 25.671. Washington, DC: FAA, 1970.

[2] SERAFIM, C. F. Modelling and simulation of actuators in damping mode to comply with flutter requirements. 2019. 102 p. Dissertation (Master of Aeronautical and Mechanical Engineering) – Instituto Tecnológico de Aeronáutica, São José dos Campos, 2019.

[3] VALDO, M. F. Servo hydraulic technology in flight control. In: INNOVATIVE ENGINEERING FOR FLUID POWER AND VEHICULAR SYSTEMS, 2012, São Paulo. Workshop [...]. São Paulo: [s. n.], 2012. Available at: https://www.cisb.org.br/images/pdf/MarioValdo.pdf. Accessed on: 14 Jul. 2021.

[4] MIZIOKA, L.S. Modelagem e análise de desempenho do servo atuador do sistema de leme de uma aeronave sob variação de temperatura. 2009. 128f. Dissertação (Mestrado – em Sistemas Aeroespaciais e Mecatrônica) - Instituto Tecnológico da Aeronáutica, São José dos Campos, 2009.

[5] SIDDERS, J. A. Thermal-hydraulic performance prediction in fluid power systems. Journal of Systems and Control Engineering, v.210, n.4, p. 231-242, 1996.

[6] CHENGGONG, L.; ZONGXIA, J. Calculation method for thermal-hydraulic system simulation. ASME Journal of Heat Transfer, v.130, issue 8, article number 084503, 2008.

[7] ADRIANO, G. F. Análise térmica de sistemas hidráulicos de aeronaves. 2010. 85 f. Dissertação (Mestrado Profissional em Engenharia Aeronáutica) – Instituto Tecnológico de Aeronáutica, São José dos Campos, 2010.

[8] ZHANG, X.; LI, J.; YIN, Y. Thermal analysis and simulation of aircraft hydraulic system. Advanced Materials Research. v. 204-210, p 1984-1989, 2011.

[9] LI, K.; LV, Z.; LU, K.; YU, P. Thermal-hydraulic modeling and simulation of the hydraulic system based on the electro-hydrostatic actuator. Procedia Engineering, v. 80, p. 272-281, 2014.

[10] SAE INTERNATIONAL. AS1241: fire resistant phosphate ester hydraulic fluid for aircraft. Warrendale: SAE, 2016. 33p.Revision D.

[11] MERRITT, H. E. Hydraulic control systems. Boston: John Wiley & Sons, 1967. 358p.

[12] VON LINSINGEN, I. Fundamentos de Sistemas Hidráulicos. 5th ed. Florianópolis: Ed. da UFSC, 2016. 398p.

[13] SAE INTERNATIONAL. 1362: aerospace hydraulic fluids physical properties. Warrendale: SAE, 2008. 57p.

[14] SONNTAG, R. E.; BORGNAKKE, C.; VAN WYLEN, G. J. Fundamentals of thermodynamics. 6th ed. Hoboken: John Wiley & Sons, 2002, 816p.

[15] KARNOPP, D. C.; MARGOLIS, D. L.; ROSENBERG, R. C. System dynamics: modeling, simulation, and control of mechatronic systems. 5th ed. Hoboken, NJ: John Wiley & Sons, 2012. 636p.

[16] BERGMAN, T. L. et al. Fundamentals of heat and mass transfer. 7th ed. New Jersey : John Wiley & Sons, 2011. 1048p.

[17] SIEMENS. LMS Imagine.Lab. Thermal hydraulic library help. AMESim Rev. 8A Leuven, BE: Siemens, 2017a.